AJRCMB Articles in Press. Published on 23-April-2015 as 10.1165/rcmb.2014-0216OC

CARM1 regulates alveolar epithelial senescence and elastase-induced emphysema susceptibility

Rim S.J. Sarker[1], Gerrit John-Schuster[1], Alexander Bohla[1], Kathrin Mutze[1], Gerald Burgstaller[1], Mark T. Bedford[3], Melanie Königshoff[1], Oliver Eickelberg[1,2], Ali Ö. Yildirim[1]

[1]Comprehensive Pneumology Center (CPC), Institute of Lung Biology and Disease, Helmholtz Zentrum München, Member of the German Center for Lung Research (DZL), [2]University Hospital of the Ludwig-Maximilians-University, Max-Lebsche-Platz 31, 81377 München, Germany, [3]Department of Molecular Carcinogenesis, The University of Texas MD Anderson Cancer Center, Smithville, TX 78957, USA

Running title: *Reduced CARM1accelerateselastase-induced emphysema*

Author Contributions: R.S.J.S., A.B., O.E. and A.Ö.Y. designed the experiments. R.S.J.S., G.J.S., K.M. and G.B. performed the experiments. M.T.B., G.B. and M.K. provided expertise and reagents. R.S.J.S., G.Y.S., O.E., and A.Ö.Y. analyzed data and wrote the manuscript.

To whom correspondence should be addressed: Ali Ö. Yildirim, Comprehensive Pneumology Center, Institute of Lung Biology and Disease, Helmholtz Zentrum München, Ingolstädter Landstraße 1, 85764 Neuherberg, Germany, Tel:0049(89)31874037; Fax: 0049(89)31872400; Email: oender.yildirim@helmholtz-muenchen.de

Copyright © 2015 by the American Thoracic Society

"This article has an online data supplement, which is accessible from this issue's table of content online at www.atsjournals.org"

ABSTRACT:

Chronic obstructive pulmonary disease (COPD) is characterized by an irreversible loss of lung function and is one of the most prevalent and severe diseases world-wide. A major feature of COPD is emphysema -the progressive loss of alveolar tissue. Coactivator-associated arginine methyltransferase-1 (CARM1) regulates histone-methylation and the transcription of genes involved in senescence, proliferation and differentiation. Complete loss of CARM1 leads to disrupted differentiation and maturation of alveolar epithelial type-II cells (ATII). We thus hypothesized that CARM1 regulates the development and progression of emphysema. To address this, we investigated the contribution of CARM1 to alveolar rarefication using the mouse model of elastase-induced emphysema *in vivo* and siRNA-mediated knockdown in ATII-like LA4 cells *in vitro*. We demonstrate that emphysema progression *in vivo* is associated with a time-dependent down-regulation of CARM1. Importantly, elastase-treated CARM1 haploinsufficient mice show significantly increased airspace enlargement (52.5±9.6 μm vs. 38.8±5.5 μm, $p<0.01$) and lung compliance (2.8±0.32 μl/cmH_20 vs. 2.4±0.4 μl/cmH_20, $p<0.04$) compared with controls. The knockdown of CARM1 in LA4 cells led to decreased SIRT1 expression (0.034±0.003 vs. 0.022±0.001, $p<0.05$), but increased expression of p16 (0.27±0.013 vs. 0.31±0.010, $p<0.5$), p21 (0.81±0.088 vs. 1.28± 0.063, $p<0.01$) and higher beta-galactosidase-positive senescent cells (50.57%±7.36 vs. 2.21%±0.34, $p<0.001$), compared with scrambled siRNA. We further demonstrated that CARM1 haploinsufficiency impairs trans-differentiation and wound

Copyright © 2015 by the American Thoracic Society

AJRCMB Articles in Press. Published on 23-April-2015 as 10.1165/rcmb.2014-0216OC

healing (32.18%±0.9512 vs. 8.769%±1.967, $p<0.001$) of alveolar epithelial cells. Overall, these results reveal a novel function of CARM1 in regulating emphysema development and premature lung aging via alveolar senescence, as well as impaired regeneration, repair and differentiation of ATII cells.

KEYWORDS

Emphysema, Coactivator-associated arginine methyltransferase 1 (CARM1), elastase-treatment, senescence, lung regeneration, alveolar type II cells (ATII)

CLINICAL RELEVANCE

Chronic obstructive pulmonary disease (COPD) is a major cause of morbidity and mortality worldwide. Emphysema, a main feature of COPD, is characterized by airspace enlargement and loss of alveolar function. Here, we show that CARM1 deficiency predisposes mice to enhanced emphysema development, by regulating alveolar epithelial cell senescence and repair. This might help to better understand the pathogenesis of emphysema as it provides an underlying mechanism to premature senescence. The development of new pharmacological intervention regulating CARM1 activity may thus prevent emphysema development and progression. Thus, CARM1 may prove to be an effective target to treat premature lung aging in emphysema patients.

Copyright © 2015 by the American Thoracic Society

INTRODUCTION

Chronic obstructive pulmonary disease (COPD) is the most common form of chronic lung disease, primarily caused by cigarette smoke, air pollution, environmental factors, aging as well as epigenetic modification. According to the World Health Organization (WHO), COPD will stand as the third leading cause of death worldwide by the year 2030 (1). COPD is characterized by chronic bronchitis, small airway remodeling and emphysema (2). The hallmark of emphysema is the destruction of alveolar structures leading to enlarged air spaces and reduced surface area (3). The underlying mechanism of emphysema development includes a protease-anti protease imbalance (4), apoptosis-proliferation imbalance of epithelial and endothelial cells (5) and oxidative stress (6). More recently, COPD has been proposed to be a disease of accelerated premature aging. It has been demonstrated that emphysema development is driven by accelerated senescence of lung cells (7, 8), but the underlying mechanism of senescence is yet to be fully elucidated.

Protein arginine methyltransferases (PRMTs) are important for cellular processes, such as the regulation of senescence, cell proliferation, differentiation and apoptosis (9, 10). The PRMT family includes 11 members classified as type I, II or III enzymes depending on their methylation pattern (asymmetric dimethylation, symmetric dimethylation or monomethylation, respectively) (11, 12). One member of this family is PRMT4, a type I enzyme, which is also called coactivator associated arginine methyltransferase 1 (CARM1). It

Copyright © 2015 by the American Thoracic Society

AJRCMB Articles in Press. Published on 23-April-2015 as 10.1165/rcmb.2014-0216OC

was originally identified as a coactivator for steroid hormone receptors (13). CARM1 methylates histone H3 and various non-histone proteins that play essential roles in transcriptional regulation, RNA splicing, and metabolism (14, 15) and enzymatic activity of CARM1 protein is necessary for its in vivo functionality (16). CARM1 has been implicated in dysregulated cell proliferation of breast cancer, prostate cancer and colorectal cancer (17-19). Importantly, the lung of CARM1 deficient mice showed defective maturation of alveolar epithelial type II cells (ATII) and impaired trans-differentiation evident by an absence of alveolar epithelial type I cells (ATI) (20, 21). Moreover, CARM1 also plays a role in regulating cellular senescence via CARM1-dependent methylation of HuR, which stabilizes SIRT1 transcripts (22, 23). HuR, an RNA binding protein is specifically methylated by CARM1mainly at Arg^{217} of its hinge region (24). In an animal model of elastase-induced emphysema as well as in a cigarette smoke induced COPD mouse model, SIRT1 deficiency led to early development of emphysema (25). Furthermore, it has been demonstrated that there is a reduction of SIRT1 expression in the lung of smoker and COPD patients (26).

We hypothesized that CARM1 deficiency is involved in emphysema development by modulating cellular senescence in the lung and aimed to analyze the functional impact of theCARM1-SIRT1 axis in emphysema development. We demonstrated that CARM1 reduction was involved in the progression of elastase-induced emphysema. We showed for the first time that CARM1 heterozygous mice developed enhanced emphysema after elastase application as apparent by airspace enlargement and a decline in lung function. In addition, CARM1 reduction promoted senescence in ATII cells via a CARM1-SIRT1 axis and CARM1 deficiency led to impaired trans-differentiation and wound healing. Taken together, our findings unraveled that reduced CARM1 expression accelerates senescence of ATII cells and enhanced emphysema susceptibility.

Copyright © 2015 by the American Thoracic Society

Results from this study have partially been previously presented as an abstract at the International Conference of the American Thoracic Society 2014.

MATERIAL AND METHODS

Animal Experiments

Female 8-10 weeks old C57BL/6 (Charles River, Sulzfeld, Germany) and CARM1 heterozygous mice (gift from Mark Bedford, University of Texas MD Anderson Cancer Center) were treated oropharyngeally with 80 U/kg body weight porcine pancreatic elastase (PPE) (Sigma, Munich, Germany). Control mice received PBS. Wild type (WT) mice were analyzed on day 2, 28, 56 and 161 and CARM1 heterozygous animals were analyzed on day 28.Experiments were repeated twice (n= 5-6).

Lung Function Measurement

Biosystem XA forced maneuvers system and FinePointe RC system (Buxco, Wilmington, USA) measured forced expiratory volume in 0.1 second (FEV0.1), forced vital capacity (FVC), functional residual capacity (FRC) and dynamic compliance (Cdyn) and tissue elastance (E).

BAL Collection, Histology

Copyright © 2015 by the American Thoracic Society

AJRCMB Articles in Press. Published on 23-April-2015 as 10.1165/rcmb.2014-0216OC

Following bronchoalveolar lavage (BAL) the right lung was snap frozen in liquid nitrogen and the left lung was fixed at 20 cm H_2O pressure with 6% paraformaldehyde (PFA) for paraffin embedding. Details in online supplement.

Quantitative Morphometry

Mean chord length (Lm) and CARM1 or SIRT1 positive stained alveolar epithelial cells were quantified using an Olympus BX51 light microscope equipped with the newCAST (Visiopharm) as described previously (27). SP-Cpositive epithelial cells were quantified by Axio Observer.Z1 microscope (Zeiss, Göttingen, Germany) with Axiovision 4.8 (Zeiss). The p16 positive cells were quantified by applying semi-quantitative manual scoring. Details in online supplement.

Quantitative Real Time PCR

Reverse transcribed cDNA was amplified with Platinum SYBR Green qPCR SuperMix (Applied Biosystems, Darmstadt, Germany) on StepOnePlus™ PCR System (Applied Biosystems) using HPRT1 as a reference gene. Primers are listed in supplement Table E1. Relative gene expression presented as $2^{\Delta}CT$ ($\Delta Ct = Ct_{reference} - Ct_{target}$) and relative change to control as $2^{\Delta\Delta Ct}$ ($\Delta\Delta Ct = \Delta Ct^{control} - \Delta Ct^{treated}$).

Western Blot

20 µg of protein was separated by SDS-PAGE, transferred onto a polyvinylidene difluoride

Copyright © 2015 by the American Thoracic Society

membrane (Bio-Rad, Munich, Germany), blocked by 5% non-fat milk and immunoblotted with anti-CARM1 (1:750, Abcam, Cambridge, UK), anti-phospho-CARM1 (1:500, Abnova, Taipei, Taiwan), anti-SIRT1 (1:1000, Millipore, Schwalbach, Germany), anti-p16 (1:200), anti-p21 (1:200, Santa Cruz, Heidelberg, Germany) and anti-T1α (1:4000, R&D, Minneapolis, Minnesota, USA) antibodies. Upon developing with Amersham ECL Prime reagent (GE Healthcare, Freiburg, Germany) the bands were detected and quantified by Chemidoc XRS system (Bio-Rad, Munich, Germany).

Cell Culture

Murine ATII-like cell line LA-4 (ATCC, Rockville, MD) was transfected with CARM1 siRNAs (Qiagen, Hilden, Germany) and incubated for 48 hours. Wound healing assay was performed on transfected cells and gap closure was determined at 0 and 16 hours using Axiovision software (Zeiss). siCARM1-transfected cells were incubated with 5% of cigarette smoke extract (CSE) containing medium for 6 hours. Senescence assay was performed using β-galactosidase staining kit (Cell signaling, Frankfurt, Germany).

Alveolar Epithelial Type II Cell Isolation

Primary ATII cells were isolated from mouse lung and cultured as previously described (28). Details in online supplement.

Statistical Analysis

Mean values ± SD are given unless stated otherwise. Student's unpaired t-test compared two groups. One-way ANOVA following Bonferroni post-test compared more than two groups, if equal variances and normal distribution was given. Analyses were conducted using GraphPad Prism 6 (GraphPad Software, La Jolla, USA).

Copyright © 2015 by the American Thoracic Society

AJRCMB Articles in Press. Published on 23-April-2015 as 10.1165/rcmb.2014-0216OC

RESULTS

Single Application of Elastase Induced Progressive Pulmonary Emphysema in Mice

To investigate the underlying mechanism of emphysema development and progression, we used the porcine pancreastic elastase (PPE)-induced mouse model of emphysema (27). Hematoxylin and eosin (H&E) stained lung histology confirmed a time dependent progression of emphysema in elastase-treated mice compared to control mice (Figure 1A). As a direct measure of emphysema severity, the airspace enlargement was quantified by a quantitative morphometry of mean chord length (Lm) using the newCAST system (Visiopharm). The elastase-induced airspace enlargement directly correlated with increasing dynamic lung compliance (Figure 1B). Continuous elevation in forced residual capacity (FRC) (Figure 1C) and decrease of both Tiffeneau index (Figure 1D) and tissue elastance (E) until day 161 were monitored by lung function tests and further confirmed elastase-induced emphysema progression in mice.

CARM1 Expression is Diminished in Emphysematous Mouse Lungs

The coactivator-associated arginine methyltransferase 1 (CARM1) is reported to be involved in lung morphogenesis, reflected by the fact that CARM1–/– neonates are unable to inflate the

Copyright © 2015 by the American Thoracic Society

lung with air due to an abnormal alveolar air space (20). CARM1 is also important in the regulation of proliferation and differentiation of alveolar epithelial cells during lung development (21). Based on these reports we assessed CARM1 expression in emphysematous lungs by qRT-PCR and immunohistochemistry. We found a significant downregulation of CARM1 at mRNA level starting from day 28 (*$p<0.05$) that continued to decrease further until day 161 (**$p<0.01$) compared to time matched PBS-treated animals (Figure 2A). The involvement of CARM1 in emphysema development was further confirmed by quantification of CARM1 stained lung sections using the newCAST system, which revealed a significantly reduced percentage of CARM1 positive alveolar epithelial cells at day 28 and day 56 (**$p<0.01$). However no differences were observed in airway epithelial cells of elastase-treated mice compared to PBS-treated animals (Figure 2B-C). Interestingly, we also detected that at day 161, PBS-treated animals showed slightly reduced CARM1 positive SP-C cells, which is probably due to an aging effect in these mice. Therefore, we analyzed the levels of phosphorylated CARM1 because phosphorylation at a specific serine moiety renders CARM1 into an inactive state (29). We observed an age-dependent increase in phosphorylation of CARM1 at day 161 in PBS-treated animals (Figure 2D-E). Furthermore, following elastase treatment, we detected a significant increase in phospho-CARM1 levels at day 161 compared to day 28 and day 56. Taken together, these data suggested that emphysema progression is associated with a reduction of CARM1 expression and activity in lung alveolar epithelial cells.

Reduced CARM1 Expression in Mouse Lung Enhanced Elastase-induced Emphysema

Since the homozygous knockout of CARM1 is lethal (20), we proceeded with CARM1 heterozygous mice to investigate its loss of function in the pathogenesis of emphysema. The level of CARM1 protein from lung homogenate was validated by Western blot (Figure 3A).

Copyright © 2015 by the American Thoracic Society

AJRCMB Articles in Press. Published on 23-April-2015 as 10.1165/rcmb.2014-0216OC

Densitometric analysis confirmed that heterozygous mice had significantly reduced CARM1 at protein level (**p<0.01) compared to wild type (WT) mice (Figure 3B). Mean linear chord length measurement of lung histology (Figure 3C) revealed a significant airspace enlargement in CARM1 heterozygous mouse lungs compared to WT animals after elastase treatment (52.5 ± 9.6 μm versus 38.8 ± 5.5 μm, **p<0.01) at day 28 (Figure 3C-D). No difference in either airspace enlargement (22.28 μm ± 1.161 vs. 23.37 μm ± 0.8792) or lung compliance (0.001374 μl/cmH_20 ± 0.00004710 vs. 0.001391 μl/cmH_20 ± 0.0001266) was observed between WT and CARM1 heterozygous mice after PBS treatment. The higher degree of elastase-induced emphysema was also evident by a significant increase of dynamic lung compliance in CARM1 heterozygous mice compared to elastase-treated WT mice (2.8 ± 0.32 μl/cmH_20 vs. 2.4 ± 0.4 μl/cmH_20, *p<0.05) (Figure 3E). Our findings showed for the first time that CARM1 deficiency predisposed mice to a higher susceptibility of elastase-induced emphysema.

Reduced CARM1 Contributed to Senescence of Lung Alveolar Epithelial Cells

Previous studies reported that senescence of lung alveolar epithelial cells is involved in emphysema development (7, 8) although little is known about the causative mechanism. SIRT1 is an anti-senescence gene that protects against elastase-induced emphysema via reduction of premature senescence in mice (25). Interestingly, CARM1-dependent methylated HuR is reported to stabilize SIRT1 transcript (22, 23). Therefore, we investigated whether reduced CARM1 could regulate alveolar epithelial cell senescence in emphysematous lungs by modulating SIRT1. Morphological analysis of SIRT1-stained sections (Figure 4A) revealed that elastase-treatment significantly reduced the percentage of SIRT1 positive alveolar epithelial cells in WT animals, but it was not further decreased in CARM1 heterozygous mice (Figure 4B). In addition, we also detected fewer SIRT1 positive ATII cells in PBS-treated CARM1 heterozygous mice indicating that CARM1 deficiency alone could

Copyright © 2015 by the American Thoracic Society

regulate SIRT1 level in ATII cells (69.66% ± 4.55 vs. 56.92% ± 1.99, *p<0.05). When lung homogenate was analyzed by western blot, SIRT1 was shown to be downregulated in emphysematous lungs. Densitometry revealed a significant reduction in SIRT1 expression in CARM1 heterozygous mice although elastase treatment did not show further SIRT downregulation in heterozygous mice (Figure 4C). It is likely that the SIRT1 alteration in alveolar epithelial cells is being masked by other lung cell types expressing SIRT1. Several authors reported that besides stabilizing SIRT1, CARM1-dependent methylation can also destabilize transcripts of p16, which is a hallmark marker for senescence (22, 30, 31). Quantifying p16 stained sections (Figure 4D) revealed that elastase treatment induced an increase in p16 positive alveolar epithelial cells in WT as well as in CARM1 heterozygous mice. Interestingly, control CARM1 heterozygous mice showed a significant 2.5 fold increase in basal numbers of p16 positive alveolar epithelial cells compared to WT control animals (Figure 4D). In addition, we analyzed protein expression levels of p16 and p21 in lung homogenates by western blot. Elastase treatment increased expression of both p16 and p21 in CARM1 heterozygous mice although the change was not significant but we could confirm that the basal p16 expression was higher in heterozygous mice compared to WT animals (*p<0.05) (Figure 4E). We further confirmed that PBS-treated CARM1 deficient mice showed a considerably higher number of β-galactosidase positive alveolar epithelial cells compared to PBS-treated WT animals (Figure 4F). These results suggested that CARM1 deficiency attenuated the SIRT1-regulated anti-senescence mechanism, which therefore accounted for the increased susceptibility of heterozygous mice to elastase-induced emphysema.

CARM1 Reduction Accelerated Senescence *in vitro*

Copyright © 2015 by the American Thoracic Society

AJRCMB Articles in Press. Published on 23-April-2015 as 10.1165/rcmb.2014-0216OC

We and others previously reported (12, 21) that CARM1 is expressed by airway epithelial cells and by ATII cells in septal regions (Figure 2B). Therefore, we chose the ATII-like cell line LA-4 to study whether CARM1 could regulate senescence *in vitro.* siRNA transfection significantly reduced CARM1 expression by 70% as revealed by quantitative densitometry of western blot (Figure 5A upper panel, 5B). Next, we analyzed protein expression of SIRT1 and noticed a significant downregulation in siCARM1 transfected cells (*$p<0.05$) (Figure 5A middle panel, 5C). The finding was corroborated by a significant 1.5 fold reduction of SIRT1 mRNA compared to scrambled control as analyzed by qRT-PCR (Figure 5D). Concomitantly, we observed a significant upregulation of p16 and p21 but not p53 mRNA in siCARM1 transfected LA-4 cells (Figure 5E-G). Furthermore, siCARM1 transfected cells showed a significantly higher percentage of β–galactosidase positive cells compared to the scrambled control (50.57% ± 7.364 vs. 2.210% ± 0.3404, ***$p<0.001$) (Figure 5H-I). The number of positive cells was comparable to a positive control where cells were treated with 100 μM H_20_2 (data not shown). As cigarette smoke is the most common cause of emphysema, we further used cigarette smoke extract (CSE)-treated siCARM1-transfected LA-4 cells. In siCARM1-transfected cells stimulated with 5% CSE, the mRNA expression level of p21 was significantly upregulated compared to unstimulated siCARM1-transfected cells (*$p<0.05$) (Figure 5J). In accordance with this data, we also observed elevated β-galactosidase activity in siCARM1-transfected LA-4 cells after CSE stimulation (Figure 5K) demonstrating that senescence in CARM1 deficient cells was further augmented after CSE stimulation. These results confirmed that CARM1 reduction triggered an accelerated senescence in ATII cells by attenuating the effect of SIRT1.

CARM1 Downregulation Leads to Impaired Wound Healing and Aberrant Differentiation

Copyright © 2015 by the American Thoracic Society

Given that the reduction of CARM1 induced senescence in ATII cells, we sought to determine the impact of CARM1 on alveolar epithelial cell function and repair capacity. We designed a wound-healing assay using siCARM1-transfected LA-4 cells where the cell monolayer was scratched to induce a wound. CARM1-deficient cells exhibited a significant decrease in proliferation and migratory distance as evidenced by a 72.7% ± 12.2 (***$p<0.001$) reduction in gap closure compared with scrambled siRNA (32.18%±0.9512 vs. 8.769%±1.967) (Figure 6A, 6B). This finding suggested that reduced CARM1 led to impaired wound healing of ATII-like cells.

In vivo repair mechanisms consist of cellular regeneration, migration and differentiation. CARM1 is previously reported to regulate the differentiation of ATII into ATI cells, in the embryonic E18.5 mouse lung (21). We explored the role of CARM1 in the differentiation of adult murine cells by culturing primary ATII cells from WT animals, for 5 days under appropriate conditions. From day 3, cells started to differentiate into ATI-like cells, as demonstrated by expression of the ATI cell marker expression T1α. During ATII to ATI cell trans-differentiation CARM1 was significantly upregulated as analyzed by qRT-PCR (Figure 6C). Similarly, we also isolated and cultured primary ATII cells from CARM1 heterozygous mice. We detected a significant downreguation of T1α at protein level at day 5 in these mice compared to WT mice indicating that CARM1 deficiency might lead to impaired differentiation (Figure 6D). This indicates that CARM1 expression is associated with alveolar epithelial cell trans-differentiation processes.

Finally, we analyzed the number of SP-C positive cells in emphysematous mouse lungs. We observed an increased ratio of SP-C positive cells to the total cell nuclei in elastase-treated CARM1 heterozygous mice compared to PBS-treated heterozygous mice (Figure 6E-F).

Copyright © 2015 by the American Thoracic Society

AJRCMB Articles in Press. Published on 23-April-2015 as 10.1165/rcmb.2014-0216OC

Taken together these results suggest that the higher number of ATII cells probably resulted from impaired trans-differentiation.

DISCUSSION

The development of emphysema is purported to be influenced by premature aging/senescence of lung cells, but the underlying mechanism is unclear. Our study aimed at investigating the role of CARM1, a PRMT family member regulating cellular senescence via the anti-aging protein/histone deacetylase SIRT1, in elastase-induced emphysema in WT and CARM1 heterozygous mice. We reported for the first time that CARM1 deficiency caused enhanced emphysema by accelerating senescence via SIRT1 leading to impaired regeneration and differentiation of alveolar epithelial cells.

In order to mimic the irreversible structural changes occurring in the lungs of COPD patients even after smoking cessation (32), the elastase-induced emphysema mouse model is a useful and well-established tool. Despite its known half-life of a few hours and a turn-over rate of 99% in four days (33, 34), elastase triggers a continuous airspace enlargement and lung function decline even after stimulus cessation (27, 35). Most recently, a study monitored and described emphysema progression for 12 weeks by using morphometry and micro-computed X-ray tomography (36). We used the elastase-induced emphysema model as an alternative to

Copyright © 2015 by the American Thoracic Society

the cigarette smoke (CS) model, which takes considerably more time to induce significant pathological changes in the lung (starting from 4 months of exposure) (37). Furthermore, CS exposure of animals for up to 6 months only produces a mild disease, probably equivalent to human Global Initiative on Chronic Obstructive Lung Disease (GOLD) stage 1 or 2. In contrast, the elastase model is one of the fastest and easiest models available to study emphysema. This model can be established by a single treatment inducing progressive emphysema development that can reliably be monitored by lung function tests (35). Although the elastase model and cigarette smoke model both have demonstrated pathologically relevant emphysematous changes, the differences in injury pathway is still not completely known. Furthermore, the onset and duration of lesions differ in both models. To complement our elastase model, we performed an *in vitro* study with cigarette smoke extract (CSE) on siCARM1-treated LA-4 cells to evaluate the effect of CSE on cells with reduced CARM1. In addition, for a future study, we plan to use the CS model on SP-C-cre CARM1 mice.

In our study, we monitored elastase-induced emphysema progression in WT mice for a period of 161 days and demonstrate progressive disease severity associated with increased airspace enlargement and a decline in lung function parameters. As CARM1 was shown to be indispensable for normal lung development, specifically for alveolar proliferation and differentiation (20, 21), we were interested in its role in emphysema progression. Interestingly, CARM1 was downregulated in ATII cells of emphysematous lungs. CARM1 can be phosphorylated at a conserved serine residue (Ser-228 in human and Ser-229 in mouse) and the phosphorylation prevents CARM1 binding with the methyl donor S-adenosyl methionine (AdoMet) thus inhibiting its enzymatic activity (29, 38). We analyzed the ratio of phospho-CARM1 to CARM1 levels and observed a late effect on CARM1 phosphorylation after elastase treatment.

Copyright © 2015 by the American Thoracic Society

AJRCMB Articles in Press. Published on 23-April-2015 as 10.1165/rcmb.2014-0216OC

Furthermore, CARM1 deficient mice displayed pronounced and accelerated emphysema progression at day 28 in response to elastase treatment. Increasing evidence suggests that aging is a significant risk factor for emphysema development (39). Aging/senescence is a stress response marked by a progressive decline in the function of multiple cells and tissues (40). Recently, the lungs of smokers with emphysema were associated with overexpression of the cellular senescence marker p16 and telomere shortening in both alveolar epithelial type II (ATII) and endothelial cells (41). Furthermore, deficiency in the anti-senescence protein (SMP30) in mice promotes airspace enlargement after cigarette smoke exposure (42). Most importantly, CARM1 is reported to be downregulated in testis, thymus and heart of 24-month old aging rats (43). CARM1 reduction is also observed in replicative and H_2O_2-induced premature senescence of human diploid fibroblasts (44). Based on these reports and our initial findings, we hypothesized that diminished CARM1 levels might promote enhanced emphysema by regulating cellular senescence. Therefore, we investigated SIRT1, an NAD+-dependent lysine deacetylase functioning in multiple cellular events but most importantly in control of life-span and thus acting as an anti-senescence gene (45). In the lungs of smokers or COPD patients, SIRT1 is reported to be downregulated (26, 46). In mice, SIRT1 deficiency led to enhanced emphysema in both elastase- and cigarette smoke-induced models (25). Indeed, we observed a reduced basal level of SIRT1-positive alveolar epithelial cells in CARM1 deficient mice. CARM1 is reported to stabilize SIRT1 transcripts by CARM1-dependent methylation of HuR (23). We speculate that this intrinsic pro-senescent status of alveolar epithelial cells observed in our study resulted from decreased stabilization of SIRT1. Our *in vitro* study showing SIRT1 downregulation after siRNA-mediated CARM1 knockdown in LA-4 cells further confirmed the existence of a CARM1-SIRT1 axis in regulation of senescence, particularly in ATII cells. These results were corroborated by an increased basal level of p16 positive alveolar epithelial cells (Figure 4) in CARM1 deficient

Copyright © 2015 by the American Thoracic Society

mice and significant upregulation of p16 as well as p21 in CARM1 deficient LA-4 cells (Figure 5). These are two of the widely used senescence markers known to increase with aging in several rodent and human tissues and most importantly in alveolar epithelial cells of COPD patients (41, 47, 48). Moreover, previous studies showed CARM1-dependent post-translational methylation of HuR enhancing its association with p16 or p21 mRNA and leading to transcript degradation, whereas absence of CARM1 led to transcript stabilization (22, 24, 49). The impact of CARM1-mediated regulation on senescence was confirmed by increased numbers of β-galactosidase positive alveolar epithelial cells, which was augmented after CSE stimulation demonstrating that CARM1 deficiency could further enhance the senescence induction following injury stimulus in ATII cells.

CARM1-deficient mice were previously shown to have hyper-proliferative immature ATII cells that could not differentiate into ATI (21). In contrast, in CARM1 knockdown LA-4 cells, we observed a reduced gap closure, suggesting that CARM1 was required for wound healing after an injury induction in the lung. Furthermore, at day 5 when the isolated ATII cells were supposed to be completely differentiated into ATI cells under culture conditions, we detected a reduction of T1α at protein level in CARM1 deficient mice compared to WT mice. Thus, we speculated that CARM1 deficiency could indeed lead to impaired trans-differentiation.

However, we also showed an increased number of SP-C positive ATII cells in CARM1 deficient mice after elastase-treatment (Figure 6), which could be related to hyper-proliferation or dysregulated trans-differentiation of ATII into ATI thereby leading to an accumulation of ATII cells. It is possible that CARM1 regulates trans-differentiation of ATII cells via the Wnt signaling pathway involved in alveolar epithelial trans-differentiation (50). Activation of Wnt/β-catenin signaling during lung injury promotes alveolar epithelial

Copyright © 2015 by the American Thoracic Society

AJRCMB Articles in Press. Published on 23-April-2015 as 10.1165/rcmb.2014-0216OC

differentiation toward an ATI-like phenotype (51) and recently, downregulation of Wnt /β-catenin signaling has been implicated in parenchymal tissue destruction and impaired repair capacity in lungs of COPD patients (52). The methyltransferase domain of CARM1 can specifically interact with β-catenin and thus acts as a bona fide coactivator for Wnt/β-catenin signaling (19) indicating that CARM1-regulated Wnt pathway might be involved in alveolar epithelial differentiation. However, further study is required to elaborate how CARM1-regulated senescence could lead to impairment of alveolar epithelial trans-differentiation during emphysema development. Especially the upstream pathways regulating CARM1 via post-translational modifications might be a promising target for future investigation.

Taken together, our findings support the senescence hypothesis of emphysema development in COPD. In our current study, cellular senescence indeed contributed to the pathogenesis of emphysema via a CARM1-SIRT1-axis in ATII cells. We identified CARM1 as the upstream regulator of SIRT1 thereby regulating senescence and affecting regeneration, repair and differentiation of ATII cells. Our findings also provide an alternative strategy to treat emphysema. As there is no current treatment for the reversal of damaged lung structure seen in emphysema, arresting emphysema progression would be a more realistic goal to achieve. Pharmacological intervention might be applied to induce CARM1 or to prevent its degradation in emphysematous lungs. Thus, CARM1 may prove to be an effective target to slow down the premature lung aging process observed in COPD patients.

Copyright © 2015 by the American Thoracic Society

ACKNOWLEDGEMENTS

The authors acknowledge the help of Christine Hollauer, Jie Jia and cordially thank Dr. Thomas Mark Conlon for his constructive discussion.

Copyright © 2015 by the American Thoracic Society

AJRCMB Articles in Press. Published on 23-April-2015 as 10.1165/rcmb.2014-0216OC

REFERENCE

1. Murray CJ, Lopez AD. Measuring the global burden of disease. N Engl J Med. 2013 Aug 1;369(5):448-57.

2. Konigshoff M, Kneidinger N, Eickelberg O. TGF-beta signaling in COPD: deciphering genetic and cellular susceptibilities for future therapeutic regimen. Swiss Med Wkly. 2009 Oct 3;139(39-40):554-63.

3. McDonough JE, Yuan R, Suzuki M, Seyednejad N, Elliott WM, Sanchez PG, Wright AC, Gefter WB, Litzky L, Coxson HO, Pare PD, Sin DD, Pierce RA, Woods JC, McWilliams AM, Mayo JR, Lam SC, Cooper JD, Hogg JC. Small-airway obstruction and emphysema in chronic obstructive pulmonary disease. N Engl J Med. 2011 Oct 27;365(17):1567-75.

4. Mercer BA, Kolesnikova N, Sonett J, D'Armiento J. Extracellular regulated kinase/mitogen activated protein kinase is up-regulated in pulmonary emphysema and mediates matrix metalloproteinase-1 induction by cigarette smoke. J Biol Chem. 2004 Apr 23;279(17):17690-6.

Copyright © 2015 by the American Thoracic Society

5. Calabrese F, Giacometti C, Beghe B, Rea F, Loy M, Zuin R, Marulli G, Baraldo S, Saetta M, Valente M. Marked alveolar apoptosis/proliferation imbalance in end-stage emphysema. Respir Res. 2005 Feb 10;6:14.

6. Kanazawa H, Yoshikawa J. Elevated oxidative stress and reciprocal reduction of vascular endothelial growth factor levels with severity of COPD. Chest. 2005 Nov;128(5):3191-7.

7. Aoshiba K, Zhou F, Tsuji T, Nagai A. DNA damage as a molecular link in the pathogenesis of COPD in smokers. Eur Respir J. 2012 Jun;39(6):1368-76.

8. Tsuji T, Aoshiba K, Nagai A. Alveolar cell senescence exacerbates pulmonary inflammation in patients with chronic obstructive pulmonary disease. Respiration. 2010;80(1):59-70.

9. Bedford MT, Clarke SG. Protein arginine methylation in mammals: who, what, and why. Mol Cell. 2009 Jan 16;33(1):1-13.

10. Stein C, Riedl S, Ruthnick D, Notzold RR, Bauer UM. The arginine methyltransferase PRMT6 regulates cell proliferation and senescence through transcriptional repression of tumor suppressor genes. Nucleic Acids Res. 2012 Oct;40(19):9522-33.

11. Wolf SS. The protein arginine methyltransferase family: an update about function, new perspectives and the physiological role in humans. Cell Mol Life Sci. 2009 Jul;66(13):2109-21.

12. Yildirim AO, Bulau P, Zakrzewicz D, Kitowska KE, Weissmann N, Grimminger F, Morty RE, Eickelberg O. Increased protein arginine methylation in chronic hypoxia: role of protein arginine methyltransferases. Am J Respir Cell Mol Biol. 2006 Oct;35(4):436-43.

13. Chen D, Ma H, Hong H, Koh SS, Huang SM, Schurter BT, Aswad DW, Stallcup MR. Regulation of transcription by a protein methyltransferase. Science 1999; 284: 2174-2177.

Copyright © 2015 by the American Thoracic Society

AJRCMB Articles in Press. Published on 23-April-2015 as 10.1165/rcmb.2014-0216OC

14. Kuhn P, Chumanov R, Wang Y, Ge Y, Burgess RR, Xu W. Automethylation of CARM1 allows coupling of transcription and mRNA splicing. Nucleic Acids Res. 2011 Apr;39(7):2717-26.

15. Daujat S, Bauer UM, Shah V, Turner B, Berger S, Kouzarides T. Crosstalk between CARM1 methylation and CBP acetylation on histone H3. Curr Biol. 2002 Dec 23;12(24):2090-7.

16. Kim D, Lee J, Cheng D, Li J, Carter C, Richie E, Bedford MT. Enzymatic activity is required for the in vivo functions of CARM1. J Biol Chem. 2010 Jan 8;285(2):1147-52.

17. El Messaoudi S, Fabbrizio E, Rodriguez C, Chuchana P, Fauquier L, Cheng D, Theillet C, Vandel L, Bedford MT, Sardet C. Coactivator-associated arginine methyltransferase 1 (CARM1) is a positive regulator of the Cyclin E1 gene. Proc Natl Acad Sci U S A. 2006 Sep 5;103(36):13351-6.

18. Majumder S, Liu Y, Ford OH, 3rd, Mohler JL, Whang YE. Involvement of arginine methyltransferase CARM1 in androgen receptor function and prostate cancer cell viability. Prostate. 2006 Sep 1;66(12):1292-301.

19. Ou CY, LaBonte MJ, Manegold PC, So AY, Ianculescu I, Gerke DS, Yamamoto KR, Ladner RD, Kahn M, Kim JH, Stallcup MR. A coactivator role of CARM1 in the dysregulation of beta-catenin activity in colorectal cancer cell growth and gene expression. Mol Cancer Res. 2011 May;9(5):660-70.

20. Yadav N, Lee J, Kim J, Shen J, Hu MC, Aldaz CM, Bedford MT. Specific protein methylation defects and gene expression perturbations in coactivator-associated arginine methyltransferase 1-deficient mice. Proc Natl Acad Sci U S A. 2003 May 27;100(11):6464-8.

Copyright © 2015 by the American Thoracic Society

21. O'Brien KB, Alberich-Jorda M, Yadav N, Kocher O, Diruscio A, Ebralidze A, Levantini E, Sng NJ, Bhasin M, Caron T, Kim D, Steidl U, Huang G, Halmos B, Rodig SJ, Bedford MT, Tenen DG, Kobayashi S. CARM1 is required for proper control of proliferation and differentiation of pulmonary epithelial cells. Development 2010; 137: 2147-2156.

22. Pang L, Tian H, Chang N, Yi J, Xue L, Jiang B, Gorospe M, Zhang X, Wang W. Loss of CARM1 is linked to reduced HuR function in replicative senescence. BMC Mol Biol. 2013 Jul 9;14:15

23. Calvanese V, Lara E, Suarez-Alvarez B, Abu Dawud R, Vazquez-Chantada M, Martinez-Chantar ML, Embade N, Lopez-Nieva P, Horrillo A, Hmadcha A, Soria B, Piazzolla D, Herranz D, Serrano M, Mato JM, Andrews PW, Lopez-Larrea C, Esteller M, Fraga MF. Sirtuin 1 regulation of developmental genes during differentiation of stem cells. Proc Natl Acad Sci U S A. 2010 Aug 3;107(31):13736-41.

24. Li H, Park S, Kilburn B, Jelinek MA, Henschen-Edman A, Aswad DW, Stallcup MR, Laird-Offringa IA. Lipopolysaccharide-induced methylation of HuR, an mRNA-stabilizing protein, by CARM1. Coactivator-associated arginine methyltransferase. J Biol Chem. 2002 Nov 22;277(47):44623-30.

25. Yao H, Chung S, Hwang JW, Rajendrasozhan S, Sundar IK, Dean DA, McBurney MW, Guarente L, Gu W, Ronty M, Kinnula VL, Rahman I. SIRT1 protects against emphysema via FOXO3-mediated reduction of premature senescence in mice. J Clin Invest. 2012 Jun 1;122(6):2032-45.

26. Rajendrasozhan S, Yang SR, Kinnula VL, Rahman I. SIRT1, an antiinflammatory and antiaging protein, is decreased in lungs of patients with chronic obstructive pulmonary disease. Am J Respir Crit Care Med. 2008 Apr 15;177(8):861-70.

Copyright © 2015 by the American Thoracic Society

AJRCMB Articles in Press. Published on 23-April-2015 as 10.1165/rcmb.2014-0216OC

27. Yildirim AO, Muyal V, John G, Muller B, Seifart C, Kasper M, Fehrenbach H. Palifermin induces alveolar maintenance programs in emphysematous mice. Am J Respir Crit Care Med. 2010 Apr 1;181(7):705-17.

28. Konigshoff M, Wilhelm A, Jahn A, Sedding D, Amarie OV, Eul B, Seeger W, Fink L, Gunther A, Eickelberg O, Rose F. The angiotensin II receptor 2 is expressed and mediates angiotensin II signaling in lung fibrosis. Am J Respir Cell Mol Biol. 2007 Dec;37(6):640-50.

29. Higashimoto K, Kuhn P, Desai D, Cheng X, Xu W. Phosphorylation-mediated inactivation of coactivator-associated arginine methyltransferase 1. Proc Natl Acad Sci U S A. 2007 Jul 24;104(30):12318-23.

30. Chang N, Yi J, Guo G, Liu X, Shang Y, Tong T, Cui Q, Zhan M, Gorospe M, Wang W. HuR uses AUF1 as a cofactor to promote p16INK4 mRNA decay. Mol Cell Biol. 2010 Aug;30(15):3875-86.

31. Fujiwara T, Mori Y, Chu DL, Koyama Y, Miyata S, Tanaka H, Yachi K, Kubo T, Yoshikawa H, Tohyama M. CARM1 regulates proliferation of PC12 cells by methylating HuD. Mol Cell Biol. 2006 Mar;26(6):2273-85.

32. Hogg JC, Chu F, Utokaparch S, Woods R, Elliott WM, Buzatu L, Cherniack RM, Rogers RM, Sciurba FC, Coxson HO, Pare PD. The nature of small-airway obstruction in chronic obstructive pulmonary disease. N Engl J Med. 2004 Jun 24;350(26):2645-53.

33. Stone PJ, Pereira W, Jr., Biles D, Snider GL, Kagan HM, Franzblau C. Studies on the fate of pancreatic elastase in the hamster lung: 14C-guanidinated elastase. Am Rev Respir Dis. 1977 Jul;116(1):49-56.

34. Starcher BC. Elastin and the lung. Thorax 1986; 41: 577-585.

Copyright © 2015 by the American Thoracic Society

35. Vanoirbeek JA, Rinaldi M, De Vooght V, Haenen S, Bobic S, Gayan-Ramirez G, Hoet PH, Verbeken E, Decramer M, Nemery B, Janssens W. Noninvasive and invasive pulmonary function in mouse models of obstructive and restrictive respiratory diseases. Am J Respir Cell Mol Biol. 2010 Jan;42(1):96-104.

36. Kobayashi S, Fujinawa R, Ota F, Kobayashi S, Angata T, Ueno M, Maeno T, Kitazume S, Yoshida K, Ishii T, Gao C, Ohtsubo K, Yamaguchi Y, Betsuyaku T, Kida K, Taniguchi N. A single dose of lipopolysaccharide into mice with emphysema mimics human chronic obstructive pulmonary disease exacerbation as assessed by micro-computed tomography. Am J Respir Cell Mol Biol. 2013 Dec;49(6):971-7.

37. John-Schuster G, Hager K, Conlon TM, Irmler M, Beckers J, Eickelberg O, Yildirim AO. Cigarette smoke-induced iBALT mediates macrophage activation in a B cell-dependent manner in COPD. Am J Physiol Lung Cell Mol Physiol. 2014 Nov 1;307(9):L692-706.

38. Feng Q, He B, Jung SY, Song Y, Qin J, Tsai SY, Tsai MJ, O'Malley BW. Biochemical control of CARM1 enzymatic activity by phosphorylation. J Biol Chem. 2009 Dec 25;284(52):36167-74.

39. Ito K, Barnes PJ. COPD as a disease of accelerated lung aging. Chest. 2009;135(1):173-80. doi: 10.1378/chest.08-1419.

40. Campisi J, Andersen JK, Kapahi P, Melov S. Cellular senescence: a link between cancer and age-related degenerative disease? Semin Cancer Biol. 2011 Dec;21(6):354-9.

41. Tsuji T, Aoshiba K, Nagai A. Alveolar cell senescence in patients with pulmonary emphysema. Am J Respir Crit Care Med. 2006 Oct 15;174(8):886-93.

42. Sato T, Seyama K, Sato Y, Mori H, Souma S, Akiyoshi T, Kodama Y, Mori T, Goto S, Takahashi K, Fukuchi Y, Maruyama N, Ishigami A. Senescence marker protein-30 protects

Copyright © 2015 by the American Thoracic Society

AJRCMB Articles in Press. Published on 23-April-2015 as 10.1165/rcmb.2014-0216OC

mice lungs from oxidative stress, aging, and smoking. Am J Respir Crit Care Med. 2006 Sep 1;174(5):530-7.

43. Hong E, Lim Y, Lee E, Oh M, Kwon D. Tissue-specific and age-dependent expression of protein arginine methyltransferases (PRMTs) in male rat tissues. Biogerontology 2012; 13: 329-336.

44. Lim Y, Lee E, Lee J, Oh S, Kim S. Down-regulation of asymmetric arginine methylation during replicative and H2O2-induced premature senescence in WI-38 human diploid fibroblasts. J Biochem. 2008 Oct;144(4):523-9.

45. Guarente L, Picard F. Calorie restriction--the SIR2 connection. Cell 2005; 120: 473-482.

46. Nakamaru Y, Vuppusetty C, Wada H, Milne JC, Ito M, Rossios C, Elliot M, Hogg J, Kharitonov S, Goto H, Bemis JE, Elliott P, Barnes PJ, Ito K. A protein deacetylase SIRT1 is a negative regulator of metalloproteinase-9. FASEB J. 2009 Sep;23(9):2810-9.

47. Krishnamurthy J, Torrice C, Ramsey MR, Kovalev GI, Al-Regaiey K, Su L, Sharpless NE. Ink4a/Arf expression is a biomarker of aging. J Clin Invest. 2004 Nov;114(9):1299-307.

48. Chang BD, Watanabe K, Broude EV, Fang J, Poole JC, Kalinichenko TV, Roninson IB. Effects of p21Waf1/Cip1/Sdi1 on cellular gene expression: implications for carcinogenesis, senescence, and age-related diseases. Proc Natl Acad Sci U S A. 2000 Apr 11;97(8):4291-6.

49. Wang W, Furneaux H, Cheng H, Caldwell MC, Hutter D, Liu Y, Holbrook N, Gorospe M. HuR regulates p21 mRNA stabilization by UV light. Mol Cell Biol. 2000 Feb;20(3):760-9.

50. Marconett CN, Zhou B, Rieger ME, Selamat SA, Dubourd M, Fang X, Lynch SK, Stueve TR, Siegmund KD, Berman BP, Borok Z, Laird-Offringa IA. Integrated transcriptomic and

Copyright © 2015 by the American Thoracic Society

epigenomic analysis of primary human lung epithelial cell differentiation. PLoS Genet. 2013 Jun;9(6):e1003513.

51. Flozak AS, Lam AP, Russell S, Jain M, Peled ON, Sheppard KA, Beri R, Mutlu GM, Budinger GR, Gottardi CJ. Beta-catenin/T-cell factor signaling is activated during lung injury and promotes the survival and migration of alveolar epithelial cells. J Biol Chem. 2010 Jan 29;285(5):3157-67.

52. Kneidinger N, Yildirim AO, Callegari J, Takenaka S, Stein MM, Dumitrascu R, Bohla A, Bracke KR, Morty RE, Brusselle GG, Schermuly RT, Eickelberg O, Konigshoff M. Activation of the WNT/beta-catenin pathway attenuates experimental emphysema. Am J Respir Crit Care Med. 2011 Mar 15;183(6):723-33.

FOOTNOTES

*This work was supported by the Helmholtz Association.

Copyright © 2015 by the American Thoracic Society

AJRCMB Articles in Press. Published on 23-April-2015 as 10.1165/rcmb.2014-0216OC

FIGURE LEGENDS

Figure 1. Analysis of elastase-induced emphysema progression. Emphysema was induced in wild type C57BL/6 mice via oropharyngeal application of porcine pancreatic elastase (PPE) of 80 U/kg body weight in 80 µl volume and analyzed on indicated days. Mean chord length (Lm) was quantified by stereological analysis system, newCAST to determine airspace enlargement. Lung function was performed on anesthetized mice using Buxco forced maneuvers system. (A) Representative histological images from H&E stained lung sections. Scale bar: 200 µm. (B) Positive correlation between dynamic compliance and Lm. Lung function tests. (C) Functional Residual Capacity, FRC. (D) Tiffeneau-index, FEV0.1/FVC where FEV is Forced Expiratory Volume in 0.1 second and FVC is Forced Vital Capacity. (E) Tissue elastance, *$p<0.05$, **$p<0.01$, ***$p<0.001$, 1-way ANOVA followed by Bonferroni post-test, PBS vs. elastase-treated animals. Data presented are mean ± SD. The experiments were repeated twice (n=5-6).

***Figure 2*. Downregulation of CARM1 expression in elastase-induced emphysematous mouse lung.** (A) CARM1 expression at mRNA level in elastase-treated mouse lung compared to PBS treated control animals at day 2, 28, 56 and 161. The RNA was extracted from whole

Copyright © 2015 by the American Thoracic Society

lung homogenate and the reverse-transcribed cDNA was amplified by quantitative real time PCR (qRT-PCR). (B) Representative images from immunofluorescence double staining using antibodies against CARM1 (1:150) and ATII-specific marker, SP-C (1:100). Green: SP-C positive ATII cells, Red: CARM1 positive cells, Yellow (merged): CARM1 and SP-C double positive ATII cells. (Scale bar: 10 μm). (C) Quantification of CARM1 positive alveolar epithelial cells by newCAST stereology system. (D) Representative western blot for levels of phospho-CARM1 in lung homogenate. β-actin was used as loading control. The size of each band is indicated on the right. (E) Densitometric analysis of western blot for phopspho-CARM1, *$p<0.05$, **$p<0.01$, student's t-test, PBS vs. elastase treated animals. Data presented are mean ± SD. The experiments were repeated twice (n=5-6).

***Figure 3*. Enhanced airspace enlargement and increased lung function impairment in elastase-induced CARM1 heterozygous mice.** Mice were analyzed on day 28 after elastase induction. (A) CARM1 expression at protein level in homogenate analyzed by western blot. (B) Densitometry of the blot, **$p<0.01$, student's t-test, WT vs. CARM1 heterozygous animals. (C) Lm quantified by stereological analysis system, newCAST. (D) Representative histological images from H&E stained lung sections. Scale bar: 100 μm. (E) Elastase-induced alterations in lung compliance, *$p<0.05$, student's t-test vs. elastase-treated CARM1 heterozygous animals. WT=Wild type; Het=Heterozygous. Data presented are mean ± SD. The experiments were repeated twice (n=4-7).

***Figure 4*. Loss of anti-senescence SIRT1 and accumulation of senescence marker p16 in alveolar epithelial cells of CARM1 heterozygous mice.** (A) Representative images from immunofluorescence double staining using antibodies against SIRT1 (1:100) and ATII-specific marker, SP-C. Green: SP-C positive ATII cells, Red: SIRT1 positive cells, Yellow

Copyright © 2015 by the American Thoracic Society

AJRCMB Articles in Press. Published on 23-April-2015 as 10.1165/rcmb.2014-0216OC

(merged): SIRT1 and SP-C double positive ATII cells. Only the region of interest is shown. Scale bar: 10 μm. (B) Stereological quantification of SIRT1 positive alveolar epithelial cells by newCAST system. Red: positive stain, black: negative stain. (C) Representative blot for SIRT1 expression at protein level in lung homogenate and its densitometric analysis. β-actin was used as loading control. (D) Representative lung sections stained with anti-p16 Ab (1:50). Scale bar: 20 μm ~~(E)~~ and semi-quantitative manual scoring of p16 positive alveolar epithelial cells. (E) Representative Western blots and densitometric analysis for p16 (1:200) and p21 (1:200) protein levels in lung homogenate. (F) Representative lung sections stained with antibody against β-galactosidase (1:50). Scale bar: 20 μm. Red arrow indicates β-gal positive alveolar epithelial cells, *p<0.05, **p<0.01, student's t-test, wild type vs. CARM1 heterozygous mice. WT= Wild type; Het= Heterozygous. Data presented are mean ± SD, The experiments were repeated twice (n=4-7).

Figure 5*. CARM1 reduction accelerated senescence in ATII-like cell line LA-4.** Cells were transfected with CARM1 specific siRNA (siCARM1-2 or siCARM1-5) or non-specific scrambled siRNA (Scr) for 48 hours and harvested for RNA/protein analysis or incubated overnight with β-galactosidase staining solution. Untreated cells were taken as medium control (Co). (A) Representative Western blot showing CARM1 (upper lane) and SIRT1 (middle lane) at protein level. β-actin used as loading control (lower lane). B-C: Densitometric analysis of the blot for (B) CARM1 and (C) SIRT1 compared to β-actin, *p<0.05, **p<0.01, student's t-test, siCARM1-5 vs. Scr. (D) SIRT1 expression at mRNA level, *p<0.05, 1-way ANOVA. E-G: mRNA expression of (E) p16, (F) p21 and (G) p53, *p<0.05, **p<0.01, 1-way ANOVA. (H) Representative images from β-galactosidase assay. Scale bar: 2 μm. (I) Quantification of β-galactosidase positive cells from total 300 cells in10 random fields/well in 24-well plate,p<0.001, 1-way ANOVA. Data were from three

Copyright © 2015 by the American Thoracic Society

independent experiments. (J) The mRNA expression level of p21 inLA-4 cells treated with or without 5% of cigarette smoke extract (CSE). The cells were treated with CSE for 6 hours. (K) Representative images of β-galactosidase assay and quantification of β-gal positive cells treated with siCARM1 and/or 5% CSE. Scale bar: 2 μm, *p<0.05, ***p<0.001, student's t-test vs. siCARM1 treated with 5% CSE. Data represented as means ± SD. Data were from two independent experiments.

Figure 6. **CARM1reduction impaired wound healing in LA-4 cells and trans-differentiation of alveolar epithelial cells.** (A) Wound healing assay performed in confluent cultures of siCARM1-5 transfected LA-4 cells using a pipette tip. Scale bar: 200 μm. (B) Quantification of gap closure determined 16 hours after injury, ***p<0.001, 1-ANOVA. Data were from three independent experiments. (C) CARM1 mRNA expression during differentiation of isolated primary ATII cells into an ATI-like phenotype in culture at indicated days (d), *p<0.05, 1-way ANOVA, Dunnett's multiple comparison test vs. d1, n=3. (D) Representative Western blot for protein levels of CARM1 and T1α at indicated days of culture of isolated primary ATII cells from WT and CARM1 heterozygous animals. (E) Representative immunofluorescence images showing SP-C (green) positive alveolar epithelial cells on lung sections from WT or CARM1 heterozygous mice treated with either PBS or elastase. DAPI (blue) used as nuclear staining. Scale bar: 50 μm. (F) Stereological quantification of SP-C positive alveolar epithelial cells to total number of nuclei, **p<0.01, 1-way ANOVA, PBS vs. elastase-treated CARM1 heterozygous animals. Data represented as means ± SD. Data from two independent experiments.

Copyright © 2015 by the American Thoracic Society

AJRCMB Articles in Press. Published on 23-April-2015 as 10.1165/rcmb.2014-0216OC

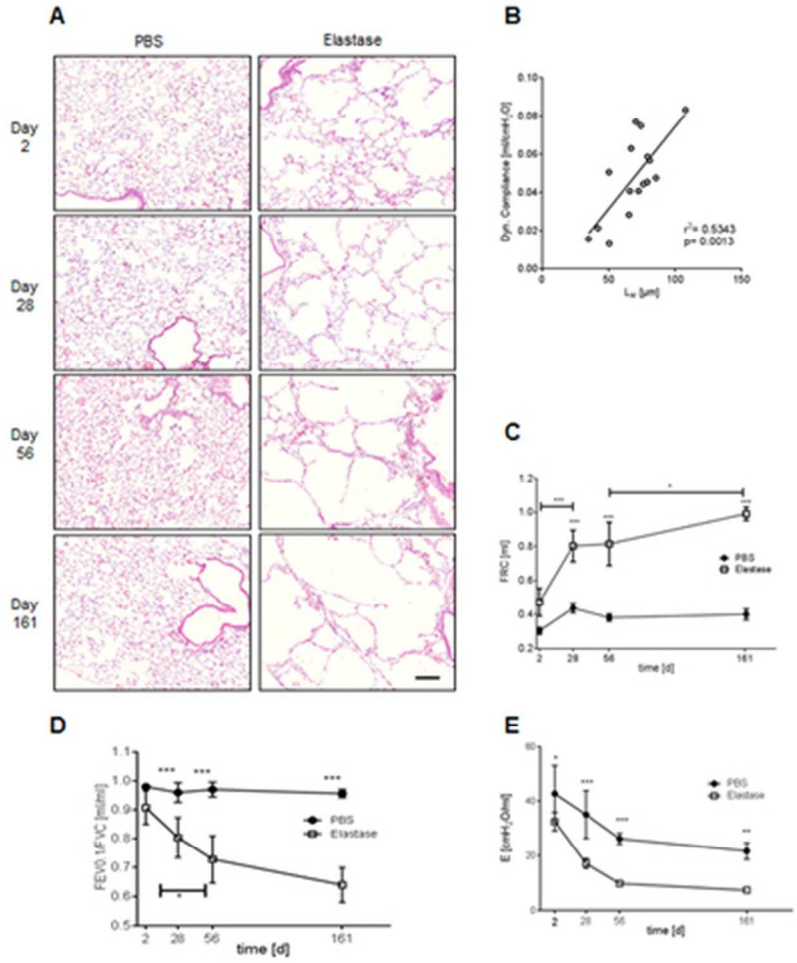

17x20mm (600 x 600 DPI)

Copyright © 2015 by the American Thoracic Society

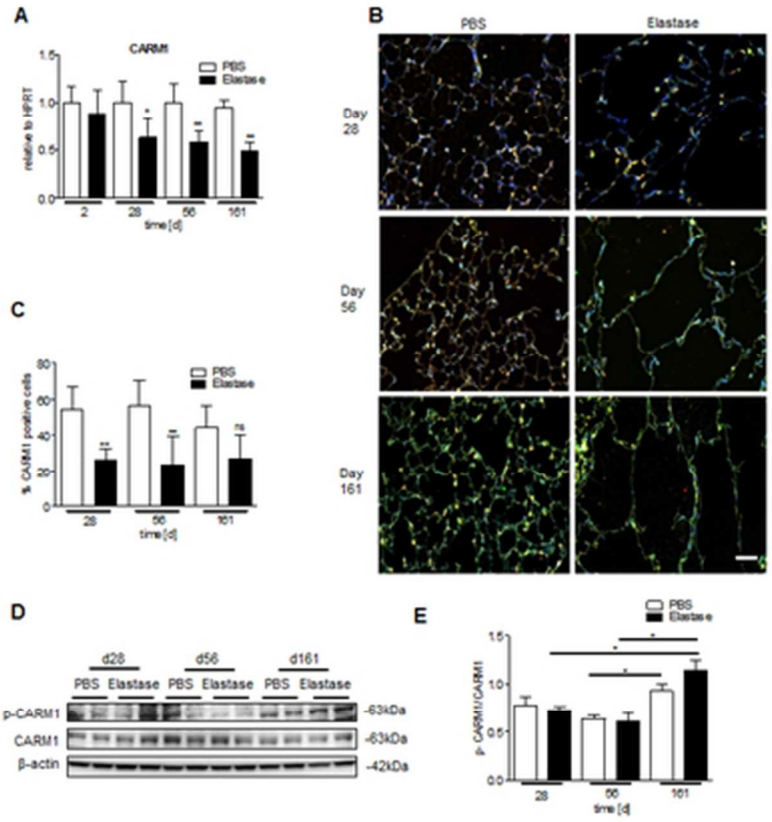

16x17mm (600 x 600 DPI)

Copyright © 2015 by the American Thoracic Society

AJRCMB Articles in Press. Published on 23-April-2015 as 10.1165/rcmb.2014-0216OC

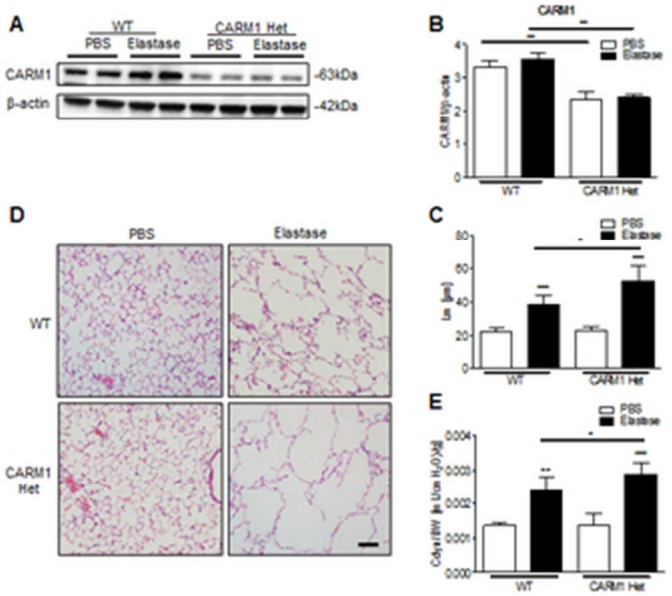

16x18mm (600 x 600 DPI)

Copyright © 2015 by the American Thoracic Society

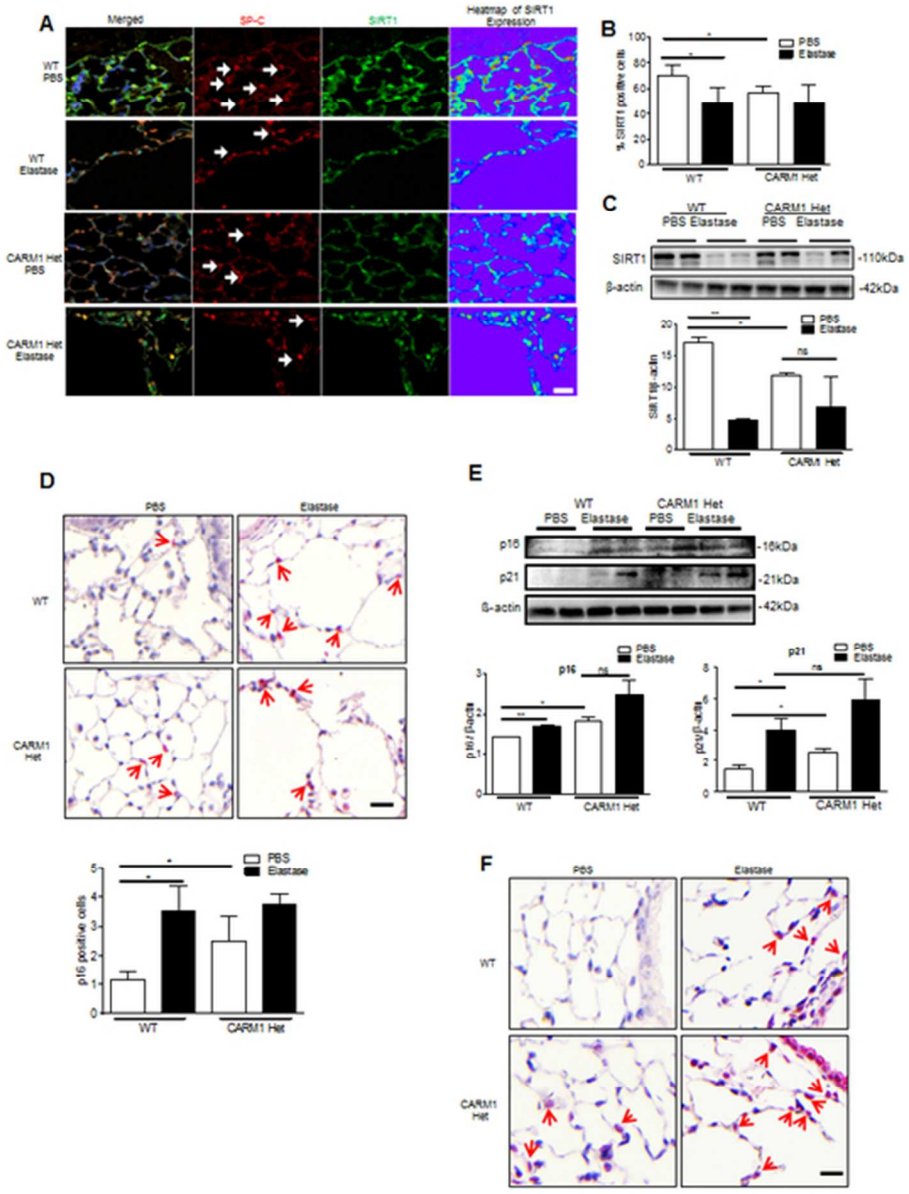

23x30mm (600 x 600 DPI)

Copyright © 2015 by the American Thoracic Society

AJRCMB Articles in Press. Published on 23-April-2015 as 10.1165/rcmb.2014-0216OC

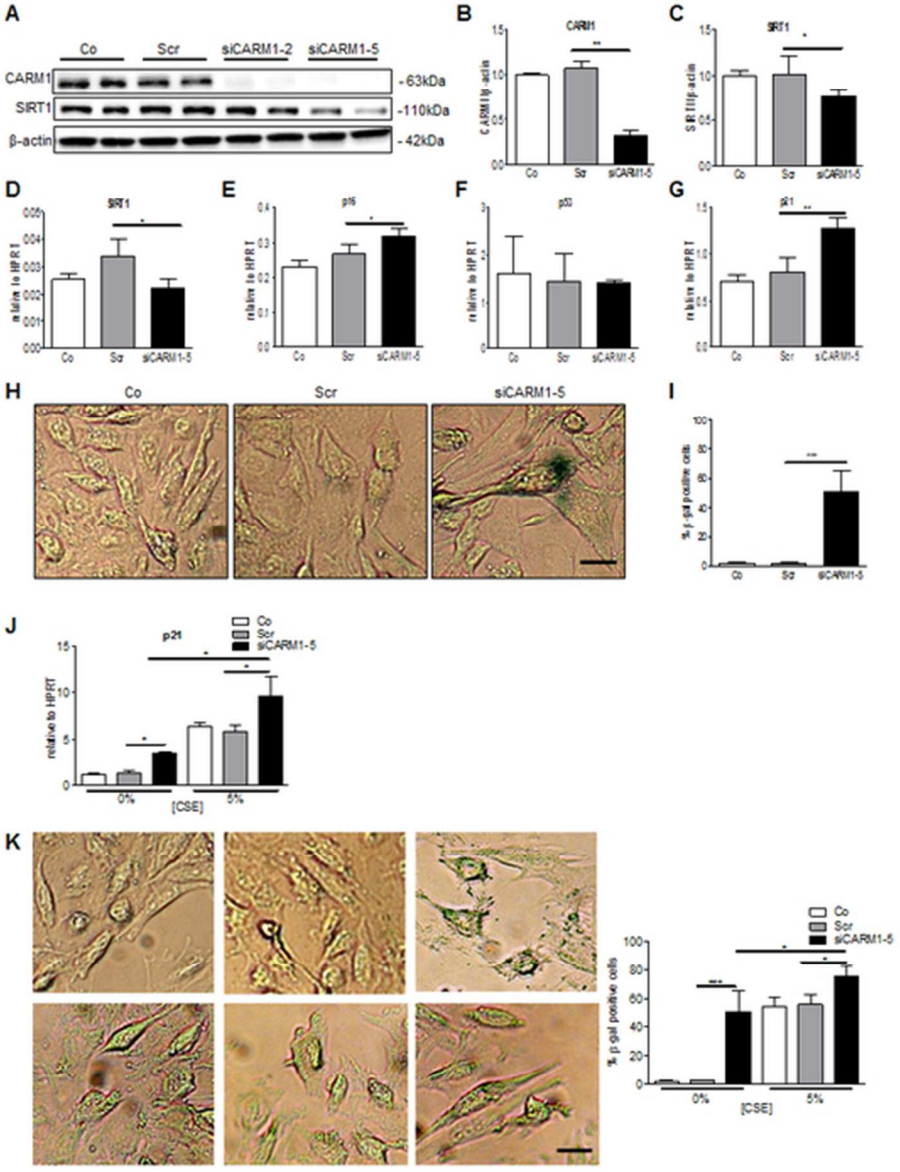

23x30mm (600 x 600 DPI)

Copyright © 2015 by the American Thoracic Society

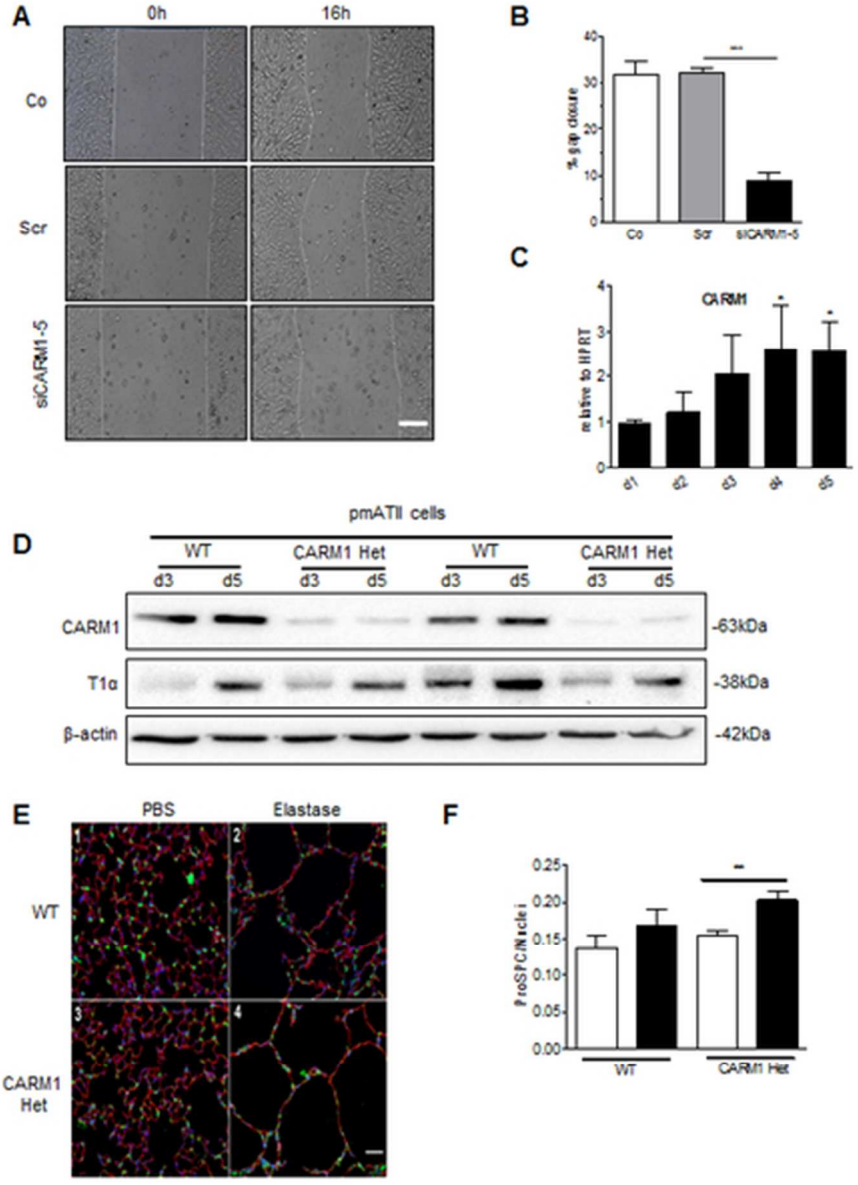

18x25mm (600 x 600 DPI)

Copyright © 2015 by the American Thoracic Society

AJRCMB Articles in Press. Published on 23-April-2015 as 10.1165/rcmb.2014-0216OC

ONLINE DATA SUPPLEMENT

CARM1 regulates alveolar epithelial senescence and elastase-induced emphysema susceptibility

Rim S.J. Sarker, Gerrit John-Schuster, Alexander Bohla, Kathrin Mutze, Gerald Burgstaller, Mark T. Bedford, Melanie Königshoff, Oliver Eickelberg, Ali Ö. Yildirim

Copyright © 2015 by the American Thoracic Society

MATERIAL AND METHODS

Animal Experiments

Eight to ten weeks old pathogen-free female C57BL/6 mice were obtained from Charles River Laboratories (Sulzfeld, Germany). The CARM1 heterozygous mice were generously provided from Mark Bedford (20) and maintained on a C57BL/6N background. Mice were housed in rooms maintained at constant temperature and humidity with a 12 hour light cycle and were allowed to access rodent laboratory chow and water *ad libitum*. All animal experiments were performed following recommendations in the Guide for the Care and Use of Laboratory Animals of the National Institutes of Health. The protocol was approved by the ethics committee of the regional governmental commission of animal protection. Animals were treated with an oropharyngeal application of porcine pancreatic elastase (PPE) (Sigma; Munich, Germany) at 80 U/kg body in 80 µl volume or PBS as vehicle control (n= 5-6). Wild type mice were analyzed on day 2, 28, 56 and 161 and CARM1 heterozygous mice were analyzed on day 28. The experiments were repeated twice.

Immunohistochemistry

The paraffin embedded lung sections (3 µm) were deparaffinized in xylene and rehydrated in alcohol. The tissue was treated with 1.8% (v/v) H_2O_2 solution (Sigma, St. Louis, MO) for 20 minutes to block endogenous peroxidase. Heat induced epitope retrieval (30 min at 125 °C; 10 min at 90 °C) was performed in HIER Citrate Buffer (pH 6.0, Zytomed Systems) in a Decloaking chamber (Biocare Medical, Concord, CA, USA). Nonspecific binding was inhibited with a blocking antibody (Biocare Medical). Tissue sections were incubated overnight at 4°C with primary antibodies against CARM1 (1:150, Abcam 87910, Cambridge,

Copyright © 2015 by the American Thoracic Society

AJRCMB Articles in Press. Published on 23-April-2015 as 10.1165/rcmb.2014-0216OC

UK), SIRT1 (1:100, Millipore 7131, Schwalbach, Germany), p16 (1:50, Santa Cruz 1207, Heidelberg, Germany) and β-galactosidase (1:50, Life Technologies, Darmstadt, Germany) and incubated afterwards with an alkaline phosphatase-labeled secondary antibody (Biocare Medical) for 1 hour at room temperature. Signals were amplified by a chromogen substrate Vulcan fast red (Biocare Medical). Tissues were counterstained with hematoxylin and dehydrated in xylene.

Immunofluorescence

Lung sections were deparaffinized, rehydrated and pressure-cooked in citrate buffer followed by peroxide treatment. After incubation with blocking antibody, the tissue sections were incubated with rabbit polyclonal antibody against Pro-surfactant Protein C (1:100 SP-C, Millipore 3786, Schwalbach, Germany), CARM1 or SIRT1 followed by 1 hour incubation with donkey anti-rabbit IgG Alexa Fluor 488 labeled secondary antibody (1:250, Invitrogen, Darmstadt, Germany). For nuclear staining, the sections were incubated with 4′,6-diamidino-2-phenylindole (DAPI 1:2000, Sigma, St.Louis, USA) in PBS for 1 min at room temperature.

For the detection of two unlabeled primary antibodies from the same host species (rabbit) we used the following protocol, where all incubation steps are at room temperature: the deparaffinized lung sections were blocked with 5% BSA in PBS for 30 min. Then the lung slices were incubated with the primary antibody (Prosurfactant Protein C) for 2 hours, washed in PBS and then the first antibody was converted into a different host by incubation with a monovalent goat-anti-rabbit Fab fragment (Jackson ImmunoResearch Laboratories, West Grove, PA, USA; 1:30 in PBS) for 2 hours. The masked antibody complexes were fixed with 4% PFA/PBS for 2 min and subsequently incubated with a donkey anti-goat IgG Alexa Fluor 568 secondary antibody for 1 hour. Finally, the lung sections were stained with the rabbit

Copyright © 2015 by the American Thoracic Society

CARM1 or SIRT1 antibodies for 2 hours, washed in PBS, and stained with the secondary donkey-anti-rabbit IgG Alexa Fluor 488 antibody for 1 hour.

Quantitative Morphometry

An unbiased design-based stereology was used to analyze sections using an Olympus BX51 light microscope equipped with the new Computer Assisted Stereological Toolbox (newCAST, Visiopharm, Hoersholm, Denmark) on HE-stained lung tissue slides as previously described (Yildirim, 2010). Briefly, a statistical estimate of air space enlargement was assessed by quantifying mean linear chord length (Lm) on 30 systemic random fields of view per lung. A line grid was superimposed on lung section images taken using the 20x objective. Intercepts of lines with alveolar septa and points hitting air space were counted to calculate mean chord length, Lm as a measurement of airspace enlargement applying the formula: $Lm = \sum P_{air} \times L(p) / \sum I_{septa} \times 0.5$. P_{air} are the points of the grid hitting air spaces, L(p) is the line length per point, I_{septa} is the sum of intercepts of alveolar septa with grid lines.

To quantify the percentage of CARM1 positive alveolar epithelial cells with newCAST, 30 systemic random fields of view per lung was chosen. A frame grid was superimposed on lung section images taken using the 40x objective. Within the frame, alveolar epithelial cells either positive or negative for CARM1 staining were counted and the percentage of CARM1 positive alveolar epithelial cells was calculated. Same method was applied to calculate the percentage of SIRT1 positive alveolar epithelial cells.

Copyright © 2015 by the American Thoracic Society

AJRCMB Articles in Press. Published on 23-April-2015 as 10.1165/rcmb.2014-0216OC

To quantify p16 positive cells a semi-quantitative manual scoring system was applied. Each lung tissue stained with p16 antibody was scored on a scale from 0–5 where 0 = no positive cells and 5 = p16 positive cells present in the highest frequency.

To quantify SP-C positive cells, images were taken with an AxioObserver.Z1 (Zeiss, Göttingen, Germany) using a Plan-Apochromat 20x/0.8 M27 objective. The automated microscopy system was driven by Axiovision 4.8 (Zeiss). For each condition 5 images were taken. The acquired data sets were imported into Imaris 7.6.5 software (Bitplane). Then, the spot detection algorithm of the Imaris software was used to assign a spot for each fluorescence intensity of DAPI stained nuclei and Pro-SPC stained cells. Finally, the number of spots was read out by the Imaris' statistics module.

Senescence-associated β-galactosidase assay:

A senescence assay staining was performed on CARM1 siRNA transfected cells using a kit (Cell signaling, Frankfurt, Germany) detecting β-galactosidase activity at pH 6. Upon fixing the cells with solution containing 2% fomaldehyde and 0.2% glutaraldehyde in PBS for 10 minutes at room temperature, the cells were incubated overnight with staining solution containing 40 mM citric acid/sodium phosphate (pH 6.0), 150 mM NaCl, 2 mM $MgCl_2$, 5 mM potassium ferrocyanide, 5 mM potassium ferricyanide and 1 mg/ml of X-gal. A percentage of positive cells was determined from 300 cells counted in 10 random fields/well. Cells treated with 100 μM H_2O_2 (Sigma) for 48 hours were positive control for senescence.

Copyright © 2015 by the American Thoracic Society

Preparation of cigarette smoke extract

Research grade cigarettes 3R4F were obtained from the Kentucky Tobacco Research and Development Center at the University of Kentucky (Lexington, KY). Cigarette smoke extract (CSE) was prepared by bubbling smoke from three cigarettes into 30 ml serum-free media at a rate of 1 cigarette per 5 minutes. This stock was considered as 100% CSE extract. (37). CSE was freshly prepared for each experiment and immediately diluted before use to 5% and 10% with culture medium (Ham's F12K liquid medium, Biochrom, Berlin, Germany) supplemented with 15% FBS.

Alveolar Epithelial Type II Cell Isolation:

Primary mouse ATII cell isolation was performed as described previously (28). In brief, mouse lungs were lavaged with 500 µl sterile PBS twice and flushed through the right heart with 0.9% NaCl solution. Lungs were inflated with dispase (BD Bioscience, San Jose, CA, USA) and incubated in dispase for 45 min at RT. Subsequently lungs were minced and filtered through 100 µm, 20 µm and 10 µm nylon meshes (Sefar, Heiden, Switzerland) and centrifuged at 200 g for 10 minutes. The cell pellet was resuspended in DMEM cell culture medium (Sigma Aldrich, St. Louis, MO, USA). Negative selection for macrophages and lymphocytes was performed with antibodies against CD45 and CD16/32 (both BD Bioscience, San Jose, CA, USA). Non-adherent cells were collected and negative selection was performed for fibroblasts by adherence for 25 minutes on cell culture dishes. Cell purity was assessed by immunofluorescence staining for proSPC, panCK, T1α, CD45, CD31 and αSMA. Cells were resuspended in DMEM containing 10% FCS, 2 mM l-glutamine, 100 U/ml penicillin, and 100 g/ml streptomycin, 3.6 mg/ml glucose, and 10 mM HEPES (PAA Laboratories, Pasching, Austria) and cultured up to 5 days in a humidified atmosphere of 5% CO_2 at 37°C with a medium change at every other day.

Copyright © 2015 by the American Thoracic Society

AJRCMB Articles in Press. Published on 23-April-2015 as 10.1165/rcmb.2014-0216OC

Supplement Table

Table E1. Primers used for quantitative real time PCR

Gene	Forward primer (5'-3')	Reverse primer (5'-3')
HPRT1	CCTAAGATGAGCGCAAGTTGAA	CCACAGGACTAGAACACCTGCTAA
CARM1	GTGGGCAGACAGTCCTTCAT	GTCCGCTCACTGAACACAGA
SIRT1	CCATTAATGAGGAAAGCAATAGGC	AATACAAGGCTAACACCTTGGG
p16	TCGTGAACATGTTGTTGAGGC	CTACGTGAACGTTGCCCATC
p21	CGGTGTCAGAGTCTAGGGGA	AGAGACAACGGCACACTTTG
p53	GTCACGCTTCTCCGAAGACT	ACAGATCGTCCATGCAGTGAG

Copyright © 2015 by the American Thoracic Society